Cloud-Cover Distributions and Correlations

P. A. JONES

Macquarie University, Sydney, Australia

(Manuscript received 12 December 1990, in final form 31 October 1991)

ABSTRACT

Observations of cloud cover (in oktas or tenths) by ground-based observers have been studied to investigate the distribution of cloud-cover amounts and the correlation of cloud cover in time and space. The correlation between observations at the same station, at different times, was found to vary as an exponential of the time separation. Similarly, the correlation between observations at different stations at the same time was found to vary as an exponential of the distance between the stations. Characteristic scales of cloud variation in space and time were derived from these exponentials and the shape of the distribution (in oktas or tenths) of cloud cover was described by a shape parameter. It was found that the data show only weak correlations between these three derived parameters, although it may be expected from physical arguments that the parameters are related.

1. Introduction

Clouds are a major component of the climate system, reflecting and scattering the radiation that drives the climate and comprising part of the hydrological cycle. For climate studies, the mean cloud cover averaged for a particular area, time of day, and time of year are generally considered to show the geographic variation and the diurnal and seasonal cycles. However, the climate is a nonlinear system so that it is not sufficient to simply consider these averages; some indication of the variability in cloud cover and the distribution of the amount of cloud cover is necessary. The radiation regime of an area that alternates between clear sky and full cloud cover is not equivalent to one that always has 50% cloud cover.

The description of clouds and their effect are major uncertainties in general circulation models (GCMs) of the climate (Webster and Stephens 1984; Wetherald and Manabe 1988). Complete physical descriptions of the small-scale physical processes in clouds are not practical for GCMs, so descriptions on large grid scales must have simplified models of subgrid-scale processes. Thus, it is useful to develop empirical models from cloud observations. In particular, it is necessary to study the variability of cloud cover on space and time scales smaller than the grid scales. Satellite observations can be used (Rossow 1989), but this paper considers records from ground-based visual observations, which are expected to agree well (McGuffie and Henderson-Sellers 1990) with the two-dimensional projection of cloud onto the earth's surface.

Corresponding author address: Dr. Paul A. Jones, 8 Pelican St., Gladesville NSW 2111, Australia.

2. Cloud-cover distributions

Cloud cover is measured by observers estimating the fraction of the solid angle of the sky hemisphere covered with cloud to the nearest eighth (okta) or tenth. While there are differences in observing conventions (for different countries and over time), all schemes require 0 okta (0 tenth) to be completely clear sky and 8 oktas (10 tenths) to be complete cloud cover. That is, the smallest amount of cloud is reported as 1 okta (1 tenth) and the smallest gap in cloud cover as 7 oktas (9 tenths). This would imply that the okta bins are actually centered at 0, 0.75, 2, 3, 4, 5, 6, 7.25, and 8 eights of cloud cover, with the end bins having negligible width and bins 1 and 7 having width 1.5 times that of the other bins. For example, the 2-okta bin extends from 1.5/8 to 2.5/8 of sky cover having a center of 2/8 and a width of 1/8 but the 1-okta bin extends from just over 0/8–1.5/8 of sky cover having a center of 0.75/8 and a width of 1.5/8. The 0-okta bin extends from 0/8 to just over 0/8 and so has a center of 0/8 and a negligible width. The U.K. Meteorological Office *Observer's Handbook* (1969) uses the above convention for 0 and 8 oktas, but requires 1 okta to be less than 1/8 and 7 oktas more than 7/8 cloud cover, so that the bins are centered at 0, 0.5, 1.75, 3, 4, 5, 6.25, 7.5, and 8 eights of cloud cover. Thus, the end bins have a negligible width, and it is bins 2 and 6 that have a width of 1.5 times that of the others.

The distribution in oktas of a large number of cloud observations shows a wide range of shapes (e.g., Fig. 1). Qualitatively, the shapes vary from centrally peaked (approximately Gaussian) distributions through flat distributions to U-shaped distributions. The shapes can be skewed to high or low values so that the mean cloud $\bar{C}$ varies between stations, but stations with similar

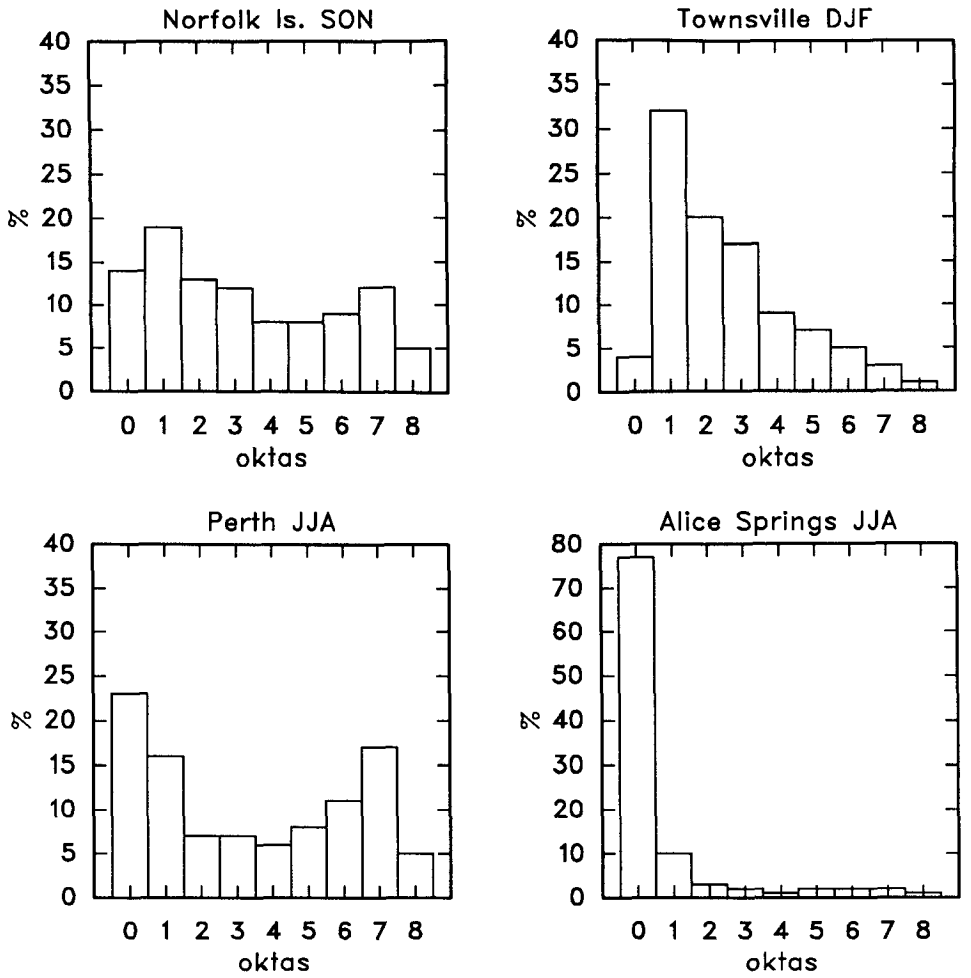

FIG. 1. The distribution in oktas of cloud cover for four Australian stations, illustrating the range of shapes of the distributions: Perth, a U-shaped distribution; Norfolk Island, a more flat distribution; Townsville, a more centrally peaked distribution; and Alice Springs, a highly skewed distribution. The data are for all times of day and for the seasons noted (3-hourly observations for 10 years, 1979–88). These plots do not show the full range of shapes; distributions for other regions, seasons, and times of day show distributions that are closer to Gaussian or more dominated by 0 and 8 oktas.

means can have different distributions, so that (at least) another parameter is needed to describe the distributions. Most simply, this can be described by differing standard deviations σ. If cloud cover is expressed as a fraction limited to the range 0–1, it can be shown that $\sigma \leqslant [\bar{C}(1 - \bar{C})]^{0.5}$. When using the pair $(\bar{C}, \sigma)$ to parameterize the distribution, the high and low values of $\bar{C}$ are always associated with low σ. Therefore, the value of σ does not give a good description of the shape of the distribution, for example, $\sigma = 0.25$ corresponds to a centrally peaked distribution if $\bar{C} = 0.5$ but a U-shaped distribution if $\bar{C} = 0.9$. A better parameter to use when comparing the shape of the distributions is the standard deviation normalized by the maximum possible (for that value of mean cloud) NS $= \sigma[\bar{C}(1 - \bar{C})]^{-0.5}$. By definition, NS $\leqslant 1$, and it is found that NS > 0.6 corresponds to a U-shaped distribution, NS ≈ 0.6 a flat distribution (for $\bar{C} \approx 0.5$, or else skewed), and NS < 0.6 a centrally peaked distribution. The parameter NS has been useful in describing how the shape of the distribution of observed cloud values compares with other parameters (see section 6).

The beta function is often used as a description of the okta distribution (Falls 1974; Henderson-Sellers 1978; Henderson-Sellers et al. 1981; Bean and Somerville 1981), where the probability function is given by

$$f(C) = C^{a-1}(1 - C)^{b-1}\Gamma(a + b)[\Gamma(a)\Gamma(b)]^{-1}$$

for $0 \leqslant C \leqslant 1$, $a > 0$, $b > 0$, where a and b are the two parameters and $\Gamma(x)$ is the gamma function. (The factor involving gamma functions is simply a normalization to make the integral of the probability unity.) Best-

fit values of a and b to fit an empirical distribution are given by

$$b^* = (1 - \bar{C})\left[\frac{\bar{C}(1 - \bar{C})}{\sigma^2} - 1\right]$$

$$a^* = \bar{C}\left[\frac{\bar{C}(1 - \bar{C})}{\sigma^2} - 1\right].$$

Comparison with the okta distribution is made by integrating $f(C)$ over the ranges of C corresponding to the okta bins. This gives a good fit (Falls 1974) provided the 0- and 8-okta bins are taken as being 0–0.5 and 7.5–8 eighths (or the corresponding ranges in tenths). Note, however, that this is not as the observing convention. If the 0- and 8-okta bins are taken as having negligible width, then the beta distribution would give zero amount in these bins.

The description in terms of a and b is equivalent to that of $\bar{C}$ and σ or ($\bar{C}$ and NS), since a and b are calculated from $\bar{C}$ and σ, but a and b have no physical significance. These two beta-distribution parameters have, nevertheless, been found useful in characterizing cloud climatologies (Henderson-Sellers 1978; Bean and Somerville 1981).

3. Cloud-cover distributions and cloud spatial variation

The shape of the distribution of cloud cover may be expected to be related to the spatial scale of variations in the clouds (Henderson-Sellers et al. 1981). If the cloud pattern varies on a scale much smaller than the observer's field of view, then different parts of the sky are uncorrelated and the cloud cover would tend toward a normal distribution around the mean cloud value. If the cloud pattern varies on a scale much larger than this field of view, then the cloud over the sky is highly correlated, leading to a U-shaped distribution (essentially no cloud and full cloud).

Qualitatively, this is shown by the change in shape of the cloud-cover distribution for satellite data as the area of "observation" is varied (Rossow 1989) and for similar data described by the beta distribution (Henderson-Sellers et al. 1981). If the shape of the cloud-cover distribution is described by the mean and standard deviation ($\bar{C}$, σ), then σ depends on the area used (Hughes and Henderson-Sellers 1983). Similar results would be obtained for fixed areas if the spatial scale of the cloud patterns varied.

Thus cloud cover could be described by two physically meaningful parameters, mean cloud and characteristic spatial scale. The Burger distribution (Burger 1985) uses such a model with C and $d_{0.99}$, where $d_{0.99}$ is the distance at which the correlation coefficient between the cloud cover at two points falls to .99. It has been found to give a good fit to the empirical distributions comparable to that of the beta distribution and a better fit if the end bins are taken as the observing convention requires. The Burger distribution is based on simulations with multiple randomly oriented sawtooth functions describing the cloud pattern. These patterns have correlation coefficient $r(s)$ given by

$$r(s) = 1 - (12/\pi)s + 3s^2$$

for $0 \leqslant s \leqslant 1$, where s is the distance in units of wavelengths of the sawtooth function. This curve is based on data from 17 stations in the midwest United States (Grantham and Boehm 1986). The cloud data presented here (section 6 and Fig. 6) give a different curve.

Values of $d_{0.99}$ have been fitted for worldwide data (Burger 1985), although not with complete global coverage. The Burger distribution has also been used to fit Canadian data (Henderson-Sellers and McGuffie 1991). It is not clear, however, whether the simulations with sawtooth functions are sufficiently realistic for the value of $d_{0.99}$, calculated from the fit to the Burger distribution, to represent the physical correlation scale of the cloud patterns. It is possible that $d_{0.99}$ is just a parameter describing the distribution and has no relation to the actual correlation scale (if any) of the cloud pattern. This point is considered below. Spatial correlation functions from cloud-cover data are considered in section 5, and the relation of the shape of the cloud-cover distribution to correlation scales is considered in section 6.

It has been argued that clouds are fractals (Mandelbrot 1983; Feder 1988) that show self-similarity over several orders of magnitude of scale (Lovejoy 1982; Welch et al. 1988; Rys and Waldvogel 1986; Cahalan and Joseph 1989) in the area–perimeter relationship. If clouds were true fractals, they would have no preferred scale, and models that attempted to fit a characteristic spatial scale would fail. Physically, there must be some scale lengths involved in clouds (at least as upper and lower limits to any fractal nature), but it is possible that the spatial scales are not sharply defined, so that fitting characteristic scales to cloud patterns would be possible but not very useful.

4. Simulations of cloud patterns

Simulations were made of cloud fields with a well-defined correlation scale to obtain the cloud-cover distributions, in order to investigate the relation between the distribution and correlation scales (see section 6), and for comparison with the Burger distribution. The two-dimensional cloud pattern was generated by a modification of the method of Gringorten (1979). An array of random numbers was smoothed with a Gaussian function to obtain an array with a specified correlation scale. Since observations of cloud cover are concerned with the presence of cloud but not its thickness, the array was truncated to two values representing clear-sky and cloud-covered pixels (Fig. 2). The curve of correlation coefficient between pixels versus separation was well defined and reproducible, with curves

FIG. 2. The simulated cloud pattern for the model that gives a well-defined scale of correlation. An array of random numbers was smoothed with a Gaussian function (to make a correlated array) and then truncated to simulate clear-sky and cloud-covered pixels. Since there is no finescale variation, the edges are sharp, and therefore the pattern does not look intuitively "cloudlike."

obtained with Gaussians of different widths w having the same shape and with correlation coefficient $r = .5$ at separation $d_{0.5} = 1.2w$. The distribution of cloud cover was simulated by sampling the arrays over a large number of independent circular areas and counting the fraction of pixels in the area that is "cloud covered." The correlation scale of the arrays and the area of "observation" were varied.

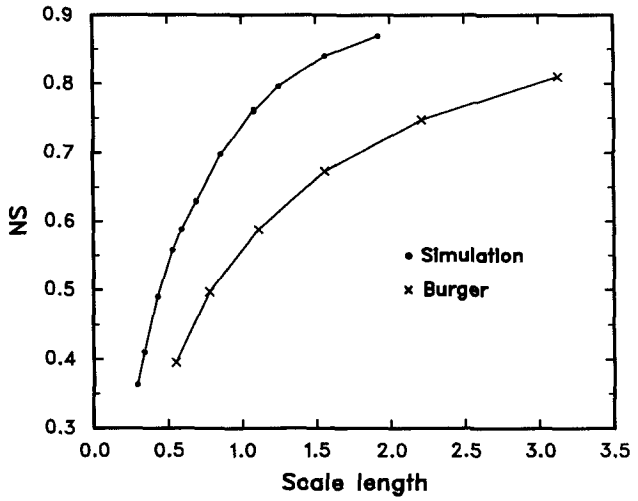

FIG. 3. The relation between the shape of the distribution of cloud-cover values and the scale of spatial correlation for the cloud patterns simulated here (e.g., Fig. 2) and for the Burger distribution. The shape is described by NS = $\sigma[\bar{C}(1 - \bar{C})]^{-0.5}$: for the simulations here $\bar{C} = 0.5$ so NS = 2σ. The scale length is $d_{0.5}$, the scale at which the correlation coefficient of the cloud pattern falls to .5; in units of the effective radius of the observation field of view, $(A/\pi)^{0.5}$.

The results confirm that the shape of the cloud-cover distribution is closely related to the ratio of the correlation scale to the observation area. If the correlation scale is small, the distribution is Gaussian-like; if the correlation scale is large, the distribution is U-shaped. This is shown in Fig. 3, where the shape of the distribution is described by NS as a function of scale length.

There is a qualitative agreement with the Burger distribution. However, a detailed comparison between these simulations and the Burger distribution shows poor quantitative agreement (Fig. 3). The correlation scales (at the $r = .5$ level) for a given shape of distribution differ by a factor of around 2 for the two models and are not even linearly related within 20%.

It is not suggested that the simulations here (Fig. 2) give a realistic model of cloud patterns. However, the fact that there are large differences compared to Burger's simulations indicates that the scale length obtained from the distributions is sensitive to the details of the simulation (Fig. 3). Thus, even if it is assumed that the cloud pattern has a well-defined scale, fitting cloud-cover observations to the Burger distribution does not accurately give this scale.

Figure 4 shows an example of a simulated cloud field that does not have a well-defined scale. The simulation is based on a Brownian relief (Mandelbrot 1983; Peitgen and Saupe 1988) obtained by multiple, randomly positioned and randomly oriented steps on a plane, a method that is used to model surfaces (e.g., mountains) as fractals for computer images (Voss 1985). The relief is truncated (as above) to give two states of clear-sky and cloud-covered pixels. The boundary is a fractal. The correlation coefficient versus separation curve varies markedly between repeated

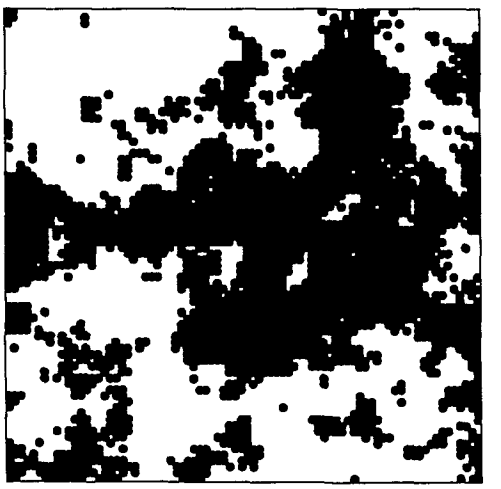

FIG. 4. The simulated cloud pattern for the fractal model, where the spatial scale is not a single, well-defined quantity. Multiple step functions of random position and angle were added into the array, and then the array was truncated as for Fig. 2. The range of spatial scales captures the intuitive appearance of clouds better than Fig. 2.

simulations and within a single simulation (i.e., there are areas with broad structure and other areas with much smaller structure). The separation at which $r = .5$ varies by an order of magnitude between simulations.

The irregular structure of the fractal model (Fig. 4) captures some of the "fluffy" appearance of clouds, which is why clouds are sometimes modeled as fractals in computer images (Peitgen and Saupe 1988), although more realistically as three-dimensional fractals with the brightness in two dimensions depending on the optical depth in the other dimension (Voss 1985). In contrast, Fig. 2 looks too regular with sharp edges.

It is useful to model clouds as irregular objects since, for example, the structure of the cloud affects the scattering of radiation that is important in parameterizing the effects of clouds in GCMs (clouds are not plane-parallel slabs) and in developing algorithms to distinguish clouds in satellite images (clouds do not have sharp edges).

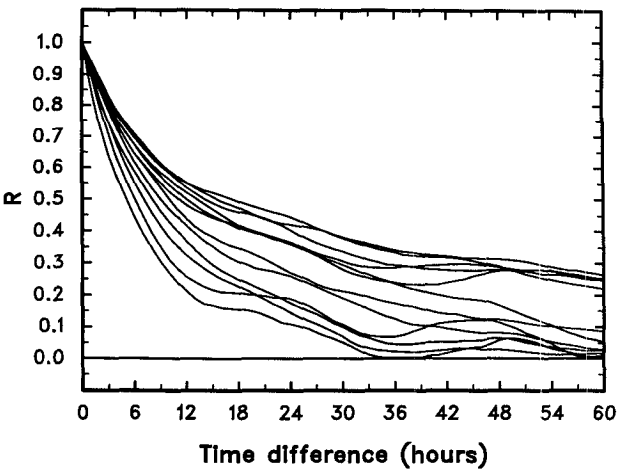

FIG. 5. The correlation coefficient r between cloud-cover observations at individual stations as a function of the time difference between the observations. The data are for Canada, but only 10 of the 154 stations are plotted (for clarity), showing a range of time scales. Note that the curves are roughly exponentials but that there are peaks of correlation at 24 and 48 h due to the diurnal cycle.

5. Cloud-cover correlations

In order to investigate the correlation in space and time of cloud cover, several different sets of observations were considered. Cloud-cover observations for 13 Australian stations (10 on the Australian continent, plus Norfolk Island, Macquarie Island, and Mawson in Antarctica), taken eight times a day for 10 years (1979–88), were obtained from the Australian Bureau of Meteorology. Some of these observations, in oktas, are used in Fig. 1. Data for Canada were obtained for 154 stations, hourly for 1 year (1985), in tenths of sky cover. This dataset was derived from the Atmospheric Environment Service, Canada, and are the same data fitted to the Burger distribution by Henderson-Sellers and McGuffie (1991). Some data were also taken from the worldwide dataset in TD13 format, obtained from the U.S. National Center for Atmospheric Research (NCAR) for New Zealand and Canada. The TD13 data confirmed the results from the other two datasets, but they are not plotted here, since the coverage of data in space and time was much more sparse than the other datasets.

The data for individual stations were analyzed to determine the correlation as a function of time separation. (The numbers in oktas and tenths were used without any correction for the definitions of 0, 1, 7, and 8 oktas or 0, 1, 9, and 10 tenths; section 2.) Figure 5 shows the curve of correlation coefficient r versus time separation Δt for 12 Canadian stations (for clarity, not all 154 stations are plotted). Due to the diurnal cycle in cloud cover, the curves show peaks at around 24 and 48 h. Apart from these peaks, the curves vary approximately as exponentials. That is, the exponential is the simplest curve, with only one free parameter, the time constant (since $r = 1$ at $\Delta t = 0$ by definition), which fits the correlation data within the expected uncertainty. Other simple curves (such as power laws) do not fit the data as well, and more complicated fits are not justified given the range of curves. For convenience, the time constant is described here by $t_{0.5}$, the time separation Δt at which $r = .5$, which is obtained by interpolation. Presumably, the different time constants represent geographic variation in cloud properties (e.g., dominant cloud type) between stations. Section 7 discusses briefly a breakup of the data by season and location, but the data used here do not include cloud type or height, only total cloud amount.

Similar curves to Fig. 5 were obtained for the Australian data, although with Δt in 3-h steps giving sparse time coverage. These time-lag autocorrelation functions are similar to those obtained by Cahalan et al. (1982), where infrared fluxes from National Oceanographic and Atmospheric Administration (NOAA) satellite data were used as an estimate for cloud.

To determine the spatial correlation of cloud cover, the data for pairs of stations were considered. The correlation coefficients between the time series for pairs of Canadian stations are plotted in Fig. 6 as a function of the separation between stations. The resulting curve is again approximately an exponential, $r = \exp(-d/\tau_d)$, so that an estimate of spatial scale τ_d can be obtained for each station pair. (This is restricted to pairs with $d < 1000$ km, since for larger separations the correlation coefficient is near zero. Similarly, there are some points with $r < 0$, due to the scatter in r, which cannot be fitted with an exponential.) Note that this is different from the model used for the Burger distri-

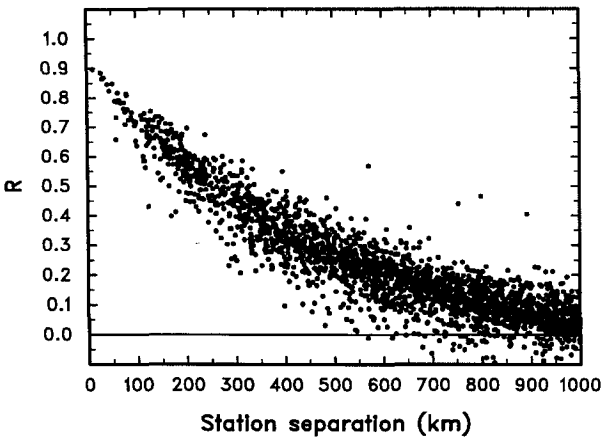

FIG. 6. The correlation coefficient r between cloud-cover observations at two stations as a function of the separation between the two stations for the Canadian data. Note that the points follow a roughly exponential curve. There are more station pairs with separation greater than 1000 km, but these are essentially uncorrelated $r \approx 0$.

bution (section 3). The Australian dataset shows similar results to Fig. 6, but the spatial coverage of stations is so sparse that there are only a few station pairs with separation $d < 1000$ km, and therefore few useful values of τ_d could be calculated.

It is expected that there is a relation between the time scale of cloud variations and the spatial scale of variations, if only because the cloud cover of a particular site changes with the movement of the cloud pattern with the prevailing winds. More fundamentally, there should be a relationship due to the underlying physics of the cloud variations, for example, convection cells. Since the scale length τ_d is determined from station pairs, a time scale was calculated for these pairs by the geometric mean of the two time constants $t_{0.5}$. The plot of scale length versus time constant (Fig. 7) shows a weak relationship (correlation coefficient $r = .32$), with the majority of points having time constant around 6 h and a large scatter in scale length and with the few points of larger time constant having a slightly larger scale length.

6. Cloud-cover distributions and correlation scales

It is also expected that the characteristic spatial scale of cloud correlations is related to the shape of the cloud-cover distribution (in oktas or tenths). This is the basis of the Burger distribution and is confirmed, qualitatively, by simulations (section 3, Fig. 3). This relationship can be tested by the results from the Canadian cloud data. The shape of the distribution is described by the parameter NS (section 2), since the possible range of the standard deviation σ depends on the mean cloud $\bar{C}$. Since the scale length τ_d was obtained from pairs of stations, for comparison NS was taken as the mean of the values for the two stations. The plot of NS versus scale length (Fig. 8) shows little correlation ($r = .20$). Thus, at least for the Canadian data, the shape of the cloud-cover distribution does not depend to a large extent on the scale length. Figures 7 and 8 may have been affected by the aggregation of $t_{0.5}$ and NS into pairs, required for the comparison with τ_d, which averages out some of the differences between stations.

The relationship between the shape of the cloud-cover distribution (NS) and the time scale $t_{0.5}$ for the Canadian stations is shown in Fig. 9. Again, the correlation is small ($r = .30$). Note that the points are individual stations not station pairs.

The lack of correlation between the parameters in Figs. 7, 8, and 9 may, in part, be due to the small range of these parameters ($t_{0.5}$, τ_d and NS) in the Canadian data. That is, the Canadian stations all show similar properties, presumably due to similar climatic types. Since the ranges are small, the scatter in parameters may be dominated by noise, and hence any relationship would be obscured. The Australian dataset has a larger range of NS and $t_{0.5}$, implying that the stations show a larger range of climatic types. The plot of NS versus time scale $t_{0.5}$ in Fig. 10 (analogous to Fig. 9) does show a clear relationship. Unfortunately, the other relationships could not be plotted for the Australian data since, as noted above (section 5), the sparse spatial

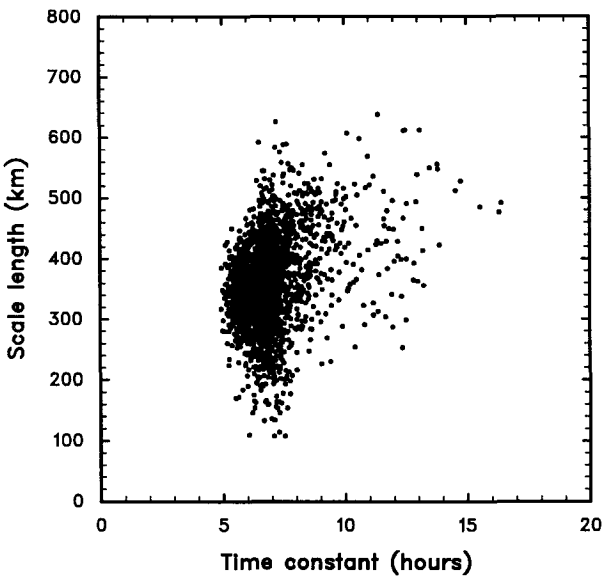

FIG. 7. The scale length (obtained from the correlation between cloud data at pairs of stations, Fig. 6) as a function of the time constant (obtained from the correlation between data at different times but the same station, Fig. 5). There is a weak tendency for long time constants to be associated with longer scale lengths, but most points lie around time constant 6–7 h with a large scatter in scale length.

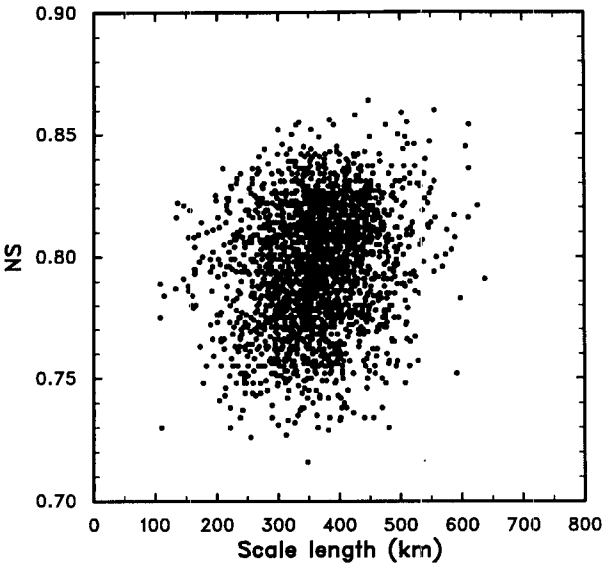

FIG. 8. The parameter describing the shape of the cloud-cover distribution $\{\mathrm{NS} = \sigma[\bar{C}(1-\bar{C})]^{-0.5}\}$ as a function of the correlation scale length. There is little relationship between the two parameters, despite the expectation (see text and Fig. 2) that they are closely linked.

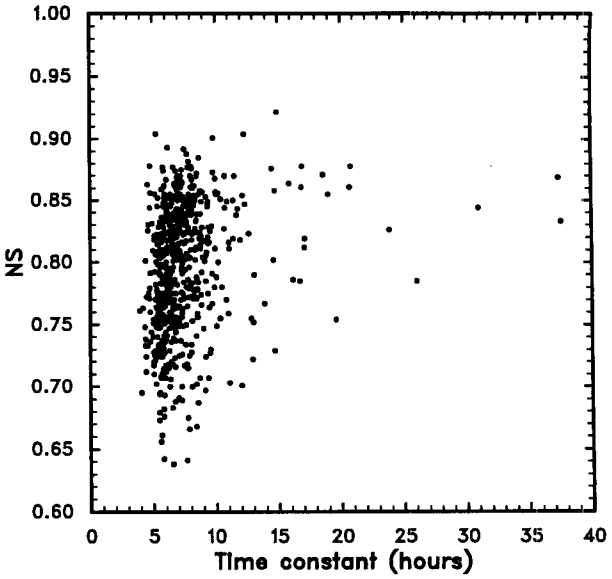

FIG. 9. The parameter describing the shape of the cloud-cover distribution (NS) as a function of the correlation time constant for the Canadian stations. There is a weak relation (similar to that in Fig. 7) with long time constants associated with high NS, although the scatter in NS is large. The data have been broken into four seasons.

coverage of stations meant few useful values of the spatial scale τ_d could be obtained.

7. Seasonal and geographic variations

The cloud-cover observations have been considered above as a single time series (hourly observations over 1 year, for the Canadian data) for a given station in order to determine the correlation scales in time and space (Figs. 5 and 6). However, cloud cover is known to vary with the diurnal and seasonal cycles so that the correlation scales may also vary with these cycles. The diurnal cycle has not been considered here, but the seasonal cycle has been investigated by considering the time series broken into four seasons [December–February (DJF), March–May (MAM), June–August (JJA), September–November (SON)]. Similarly, the histograms of cloud-cover observations have been broken into seasons to determine the seasonal cycles of $\bar{C}$ and NS. Figures 9 and 10 use these seasonal results. Figures 5–8 are given using the full years, as they are very similar to the plots using the seasonal data.

The overall seasonal cycles in parameters of mean cloud $\bar{C}$, normalized standard deviation NS, time constant $t_{0.5}$, and scale length τ_d were considered by using the values obtained for the four seasons averaged over all the Canadian stations. The cycle of $\bar{C}$ is between 6.1 (MAM) and 6.8 (SON) tenths, and the cycle of NS is between 0.74 (JJA) and 0.82 (DJF). The cycle of τ_d is between 340 (JJA) and 420 (DJF) km, indicating that NS and τ_d vary in phase (minimum during JJA). The seasonal cycle in $t_{0.5}$ is poorly determined (the seasonal variation being small compared to the differences between stations) but also has a minimum during JJA (annual range 7.1–7.8 h). The result that

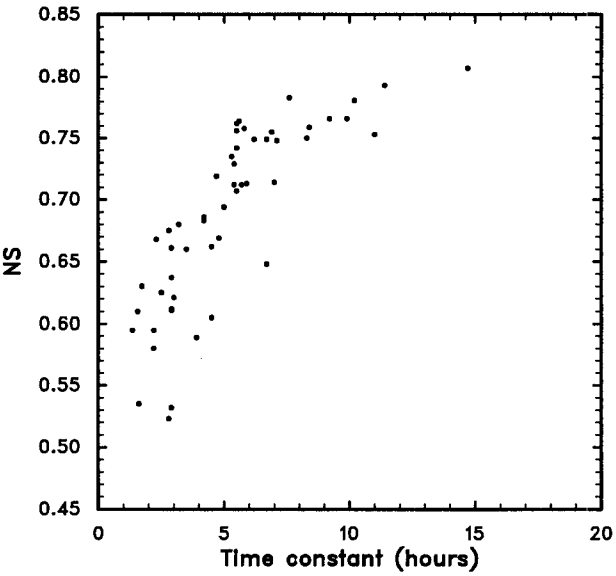

FIG. 10. The parameter describing the shape of the cloud-cover distribution (NS) as a function of the correlation time constant for the 13 Australian stations. There is a much clearer relation than in Fig. 9. The data have also been broken up into four seasons to increase the number of points.

the minima of the seasonal cycles of NS, $t_{0.5}$, and τ_d all occur during summer (JJA) is consistent with the expectation that the three parameters are related.

The geographic variation in derived parameters ($\bar{C}$, NS, $t_{0.5}$, and τ_d) was also considered by plotting the parameters against latitude and longitude or by contour plots of the data in both coordinates. There is little pattern in the variation of correlation scales $t_{0.5}$ and τ_d. Both parameters show higher values for the small number of stations north of 60°N and no clear variation in longitude. There is a similar, although weak, variation in NS with latitude, in the sense that more northerly stations show higher values, but there is a strong variation in NS with longitude with a peak around 0.83 at 90°W and falling to 0.75 on either side of the continent. The geographic variation in mean cloud $\bar{C}$ is more clear, with a decrease in cloud from south to north and a minimum in cloud of around 6.0 oktas at 100°W and an increase on either side to around 7.0 oktas. Thus, there are clear patterns in the geographic variation in cloud amount $\bar{C}$ but much less pattern to the variations in the other parameters that describe the cloud correlations.

8. Discussion

The results given above (Figs. 5 and 6) indicate that cloud-cover observations do have characteristic scales of correlation in space and time (of order a few hundred kilometers and a few hours). However, it is not clear how these results relate to the observations that show clouds have fractal structure (e.g., Lovejoy 1982), which implies spatial variation over a large range of scales. Simple inspection of cloud patterns (e.g., from satellite images) shows structure on scales ranging from thousands of kilometers down to meters.

The physical model of turbulent motions in the atmosphere is expected to lead to fractal structure. That is, large-scale motions in the atmosphere lead to a turbulent cascade where kinetic energy is translated to motions on smaller scales with self-similar properties. However, there must be an upper limit to the scale of such turbulence. Lovejoy (1982) speculates that there may be "no special or preferred horizontal length scale for atmospheric processes, except scales of the order of the size of the earth." Cloud patterns trace out these motions in the atmosphere. The results presented here on cloud correlations may indicate a preferred horizontal length scale of several hundred kilometers.

Clouds have been shown to have fractal properties [up to around 10^6 km^2 in area, Lovejoy (1982)] from the power-law behavior of the area–perimeter relation. Rys and Waldvogel (1986) and Cahalan and Joseph (1989) find that there is a break in the area–perimeter relation at the scale of a few kilometers, implying there are two fractal dimensions corresponding to scales above and below the break. Joseph and Cahalan (1990) also consider the cloud-to-cloud spacing and find that the nearest-neighbor spacing is proportional to the effective radius of the cloud (which is another example of self-similarity of the cloud patterns). It could be argued that the cloud spacing is due to a different physical process than cloud size and shape, but the proportionality above implies that the processes are closely linked. Clearly, cloud cover is not determined simply by atmospheric turbulence, but it can be argued that the patterns of clouds over short time scales (less than a few hours) and spatial scales (less than a thousand kilometers) are dominated by chaotic motions. Over long time scales, diurnal and seasonal cycles become significant, as do spatial variations due to geography (oceans, deserts, mountains, etc.).

Only the two-dimensional distribution of cloud is considered here. Clearly in the other direction (vertical), the clouds are limited to a smaller scale (of the order of 10 km, the scale height of the atmosphere) and appear at different heights depending on the cloud type. There may be some self-affinity in all three dimensions, with clouds described as multifractals (Lovejoy and Schertzer 1986, 1990), with the vertical direction scaling differently to the horizontal directions.

On some spatial scales, therefore, clouds may show fractal structure (as illustrated in Fig. 4). On large spatial scales, the cloud pattern would be more regular, but not with a single, sharply defined scale (therefore, the smooth pattern of Fig. 2 is not a good model).

The variability in the atmosphere arises from deterministic chaos, where the deterministic laws of physics (Newtonian mechanics and thermodynamics) in practice lead to unpredictability due to the sensitivity on the initial conditions (Lorenz 1963). To model atmospheric variability as represented by cloud observations properly, complex models with realistic physics are required. However, to illustrate the results here, a conceptual model is considered where the chaotic behavior is represented by a random walk. This aims to model the exponential behavior of the correlation between cloud-cover observations with a time series that has fractal structure at small scales.

The exponential form of the relation between a correlation coefficient and a time separation arises naturally from a stochastic process that varies between fixed limits. Simulations were made of such a random walk between limits (0 and 10 to simulate a time series of tenths). At each step $y(t)$ was changed by ± 1, chosen at random, so that $y(t+1) = y(t) \pm 1$, except at the limits; if $y(t) = 0$, then $y(t+1) = 0$ or 1, and if $y(t) = 10$, then $y(t+1) = 9$ or 10. The resulting curves of correlation coefficient versus time separation were roughly exponentials, that is, the correlation coefficient decreased from unity to zero in a curve that fitted an exponential within the expected scatter and was inconsistent with other simple functions such as a power law.

If $r(\Delta t) = \exp(-\Delta t/\tau)$, then the mean-square difference between values at two times is MS $= 2\sigma^2[1 - \exp(-\Delta t/\tau)]$ (where σ is the standard deviation). For short time periods, ($\Delta t < \tau$) MS $\propto \Delta t$. This approximates a one-dimensional random walk without limits (Brownian motion) that has fractal properties (Peitgen and Saupe 1988; Mandelbrot 1983), or more correctly self-affinity, since when the time is changed by factor N and the y scale is changed by factor $N^{0.5}$ the curves are similar. If the function is limited in y, the mean-square difference between values tends to a constant MS $\approx 2\sigma^2$ over long periods ($\Delta t > \tau$), the fractal structure breaks down, and the correlation coefficient tends to zero. This fractal structure is similar in the observed time series and the simulation (Fig. 11).

Figure 11a shows an example of a time series of cloud cover and Fig. 11b shows a random-walk simulation. They have similar (exponential) correlation with time separation, but the observed time series is more skewed toward high cloud-cover values with periods of consistent full cloud, whereas the simulation has a flatter distribution of values. Clearly, a simulation intended to more closely describe an observed time series would have a similar mean cloud cover $\bar{C}$, standard deviation σ, and correlation time scale. This can be done by adjusting the probabilities of the (random) steps, but the results of such simulations are not shown here since the aim is to give a simple conceptual model with as few free parameters as possible and not to reproduce the time series by varying a number of free parameters.

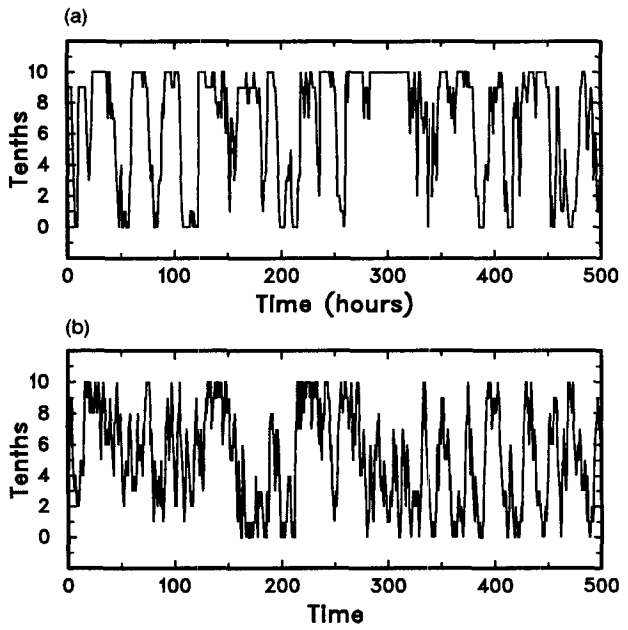

FIG. 11. (a) A time series of cloud cover, with observations every hour for 500 h. The data are in tenths from Burwash airport (Yukon Territories, Canada). (b) A simulated time series; a random walk between limits (0–10 tenths). The simulation was for 2000 steps scaled in time [to more closely match the correlation time scale of (a)] and with every third point plotted.

The one-dimensional model of time variation above could also be applied to the spatial distribution of cloud cover, but it is not clear how such a model should be generalized to the two-dimensional cloud pattern or to three dimensions, including the time variation. Such a model should have the correlation between cloud-cover values varying as an exponential (as found empirically, in this paper), with structure on a range of scales below some limit (to give self-similarity over shorter scales). A realistic model of cloud cover in space and time would need to consider the different types of cloud, since they have different fractal dimensions (Cahalan and Joseph 1989) and spatial scales.

9. Conclusions

The cloud cover for a given area cannot be adequately described simply by the mean value for that season or time of day ($\bar{C}$); the way the cloud varies around the mean should also be considered. The distribution of observed values (in oktas or tenths) shows the extent of such variation, from a U-shaped distribution with large variation to a centrally peaked distribution with little variation. This can be described by the standard deviation of the observed values, or, as used here, the standard deviation normalized by the largest possible value for that mean cloud (NS).

Comparison between observations at the same time, but at different stations, indicates that the correlation falls with distance, roughly as an exponential, with scale length around 400 km. Similar observations from the same station, but at different times, indicate that the correlation falls with time separation, also roughly as an exponential, with time constant around 6 h. These apparently well-defined scales of variation in time and space need not be inconsistent with the studies that show fractal structure in cloud patterns, since there must be some physical limit to the range of applicability of the processes that lead to a given fractal dimension.

Acknowledgments. This work was supported by a grant from the Australian Research Council. I would like to thank Ann Henderson-Sellers and Kendal McGuffie for their comments.

REFERENCES

Bean, S. J., and P. N. Somerville, 1981: Some new worldwide cloud-cover models. *J. Appl. Meteor.*, **20**, 223–228.

Burger, C. F., 1985: World Atlas of Total Sky Cover. Environmental Res. Pap. No. 927, AFGL-TR-85-0198, 112 pp. [Available from Air Force Geophysics Laboratory, Hanscom AFB, MA].

Cahalan, R. F., and J. H. Joseph, 1989: Fractal statistics of cloud fields. *Mon. Wea. Rev.*, **117**, 261–272.

——, D. A. Short, and G. R. North, 1982: Cloud fluctuation statistics. *Mon. Wea. Rev.*, **110**, 26–43.

Falls, L. W., 1974: The beta distribution: A statistical model for world cloud cover. *J. Geophys. Res.*, **79**, 1261–1264.

Feder, J., 1988: *Fractals.* Plenum Press, 283 pp.
Grantham, D. D., and A. R. Boehm, 1986: The effect of viewing aspect on climatological cloud distribution. Air Force Geophysics Laboratory, 6 pp.
Gringorten, I. I., 1979: Probability models of weather conditions occupying a line or an area. *J. Appl. Meteor.,* **18,** 957–977.
Henderson-Sellers, A., 1978: Surface type and its effect on cloud cover: A climatological investigation. *J. Geophys. Res.,* **83,** 5057–5062.
——, and K. McGuffie, 1991: Investigation of the Burger distribution to characterize cloudiness. *J. Climate,* **4,** 1181–1209.
——, N. A. Hughes, and M. Wilson, 1981: Cloud cover archiving on a global scale: A discussion of principles. *Bull. Amer. Meteor. Soc.,* **62,** 1300–1307.
Hughes, N. A., and A. Henderson-Sellers, 1983: The effect of spatial and temporal averaging on sampling strategies for cloud amount data. *Bull. Amer. Meteor. Soc.,* **64,** 250–257.
Joseph, J. H., and R. F. Cahalan, 1990: Nearest neighbor spacing of fair weather cumulus clouds. *J. Appl. Meteor.,* **29,** 793–805.
Lorenz, E. N., 1963: Deterministic nonperiodic flows. *J. Atmos. Sci.,* **20,** 130–141.
Lovejoy, S., 1982: The area–perimeter relationship for rain and cloud areas. *Science,* **216,** 185–187.
——, and D. Schertzer, 1986: Scale invariance, symmetries, fractals, and stochastic simulations of atmospheric phenomena. *Bull. Amer. Meteor. Soc.,* **67,** 21–32.
——, and ——, 1990: Multifractals, universality classes and satellite and radar measurements of cloud and rain fields. *J. Geophys. Res.,* **95,** 2021–2033.
McGuffie, K., and A. Henderson-Sellers, 1990: Are cloud amounts estimated from satellite sensor and conventional surface-based observations related? *Int. J. Remote Sensing,* **11,** 543–550.
Mandelbrot, B. B., 1983: *The Fractal Geometry of Nature.* W. H. Freeman, 438 pp.
Peitgen, H.-O., and D. Saupe, 1988: *The Science of Fractal Images.* Springer-Verlag, 312 pp.
Rossow, W. B., 1989: Measuring cloud properties from space: A review. *J. Climate,* **2,** 201–213.
Rys, F. S., and A. Waldvogel, 1986: Fractal shapes of hail clouds. *Phys. Rev. Lett.,* **56,** 784–787.
U.K. Meteorological Office, 1969: *Observer's Handbook.* Her Majesty's Stationery Office, 221 pp.
Voss, R. F., 1985: Random fractal forgeries, *Fundamental Algorithms for Computer Graphics.* R. A. Earnshaw, Ed., Springer-Verlag, 805–835.
Webster, P. J., and G. I. Stephens, 1984: Cloud–radiation interaction and the climate problem, *The Global Climate.* J. T. Houghton, Ed., Cambridge University Press, 63–78.
Welch, R. M., K. S. Kuo, B. A. Weilecki, S. K. Sengupta, and L. Parker, 1988: Marine stratocumulus cloud fields off the coast of southern California observed by Landsat imagery. I: Structural characteristics. *J. Appl. Meteor.,* **27,** 341–362.
Wetherald, R. T., and S. Manabe, 1988: Cloud feedback processes in a general circulation model. *J. Atmos. Sci.,* **45,** 1397–1415.